Supporting information

Broadband Polarization-Sensitive Photodetector and Infrared Encoder Based on High Crystallinity 1D $Bi_2(Se,S)_3$ Ternary Nanowires

Yu Zhang[a], Wenhao Fan[a], Weijie Bai[a], Wei Yan[b], Xinjian Liu[a], Yanxia Li[a], Mengyang Li[a], Jiayu Zhao[a], Jin Zhang[a], Shougen Yin[a] and Hui Yan[a,*]

[a] Key Laboratory of Display Materials and Photoelectric Devices (Ministry of Education), Tianjin Key Laboratory of Photoelectric Materials and Devices, National Demonstration Center for Experimental Function Materials Education, School of Materials Science and Engineering, Tianjin University of Technology, Tianjin 300384, China

[b] School of Science, Nanjing University of Posts and Telecommunications, Nanjing 210023, China

E-mail: H. Yan: yanhui581@163.com; yanhui@tjut.edu.cn.

ORCID: Hui Yan: 0000-0001-7902-458X

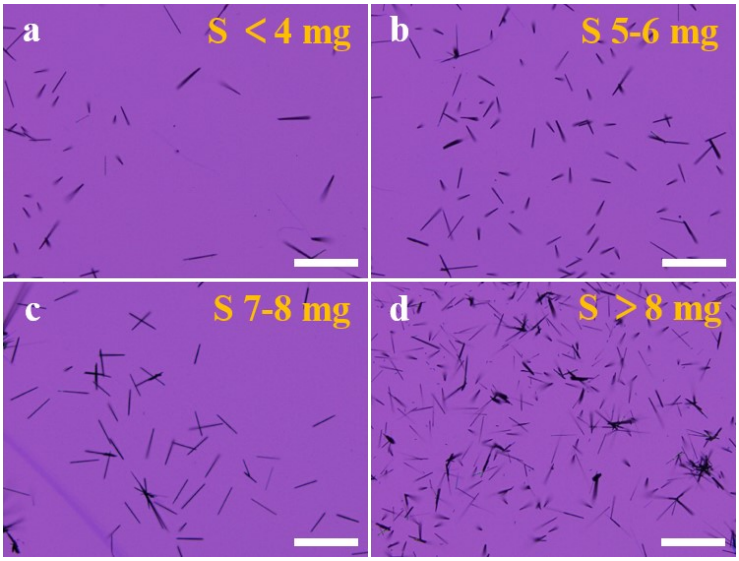

Fig. S1 OM images of $Bi_2(Se,S)_3$ nanowires grown with different S amount (a)＜4 mg, (b) 5-6 mg, (c) 7-8 mg, (d) ＞8mg. The scale bar is 100 μm.

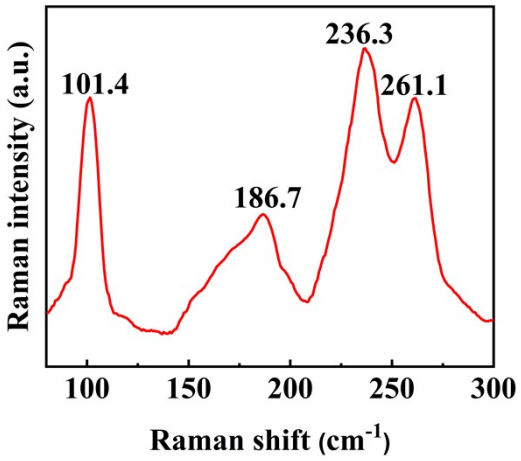

Fig. S2 Raman spectrum of Bi_2S_3 nanowire.

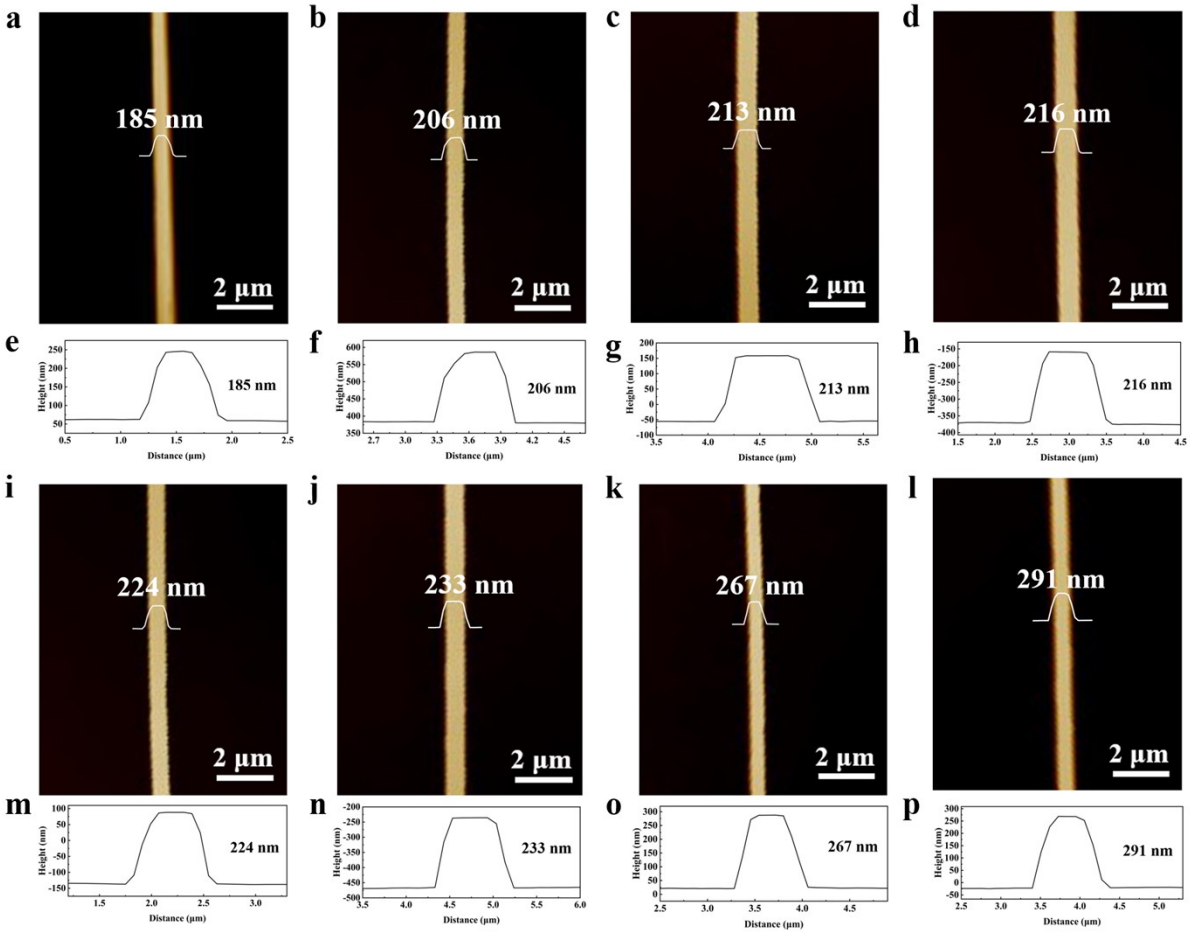

Fig. S3 (a-d, i-l) AFM images of $Bi_2(Se,S)_3$ nanowires grown on SiO_2/Si substrate. (e-h, m-p) Height distribution profiles corresponding to the above AFM images.

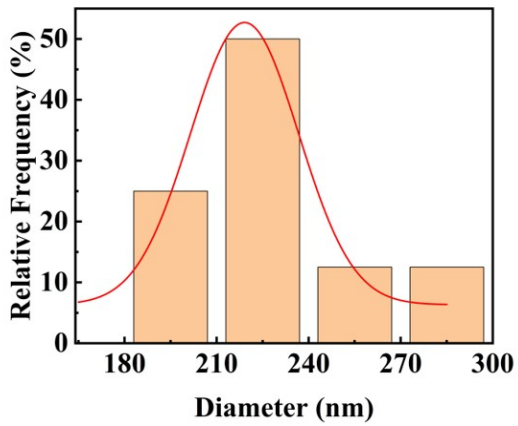

Fig. S4 Statistical distribution of nanowire diameter.

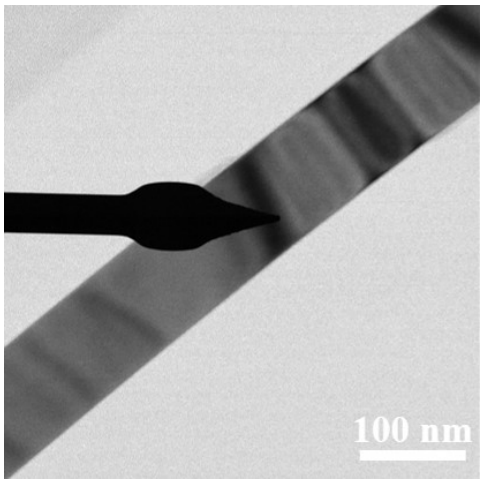

Fig. S5 Low-magnification TEM image of a typical $Bi_2(Se,S)_3$ nanowire.

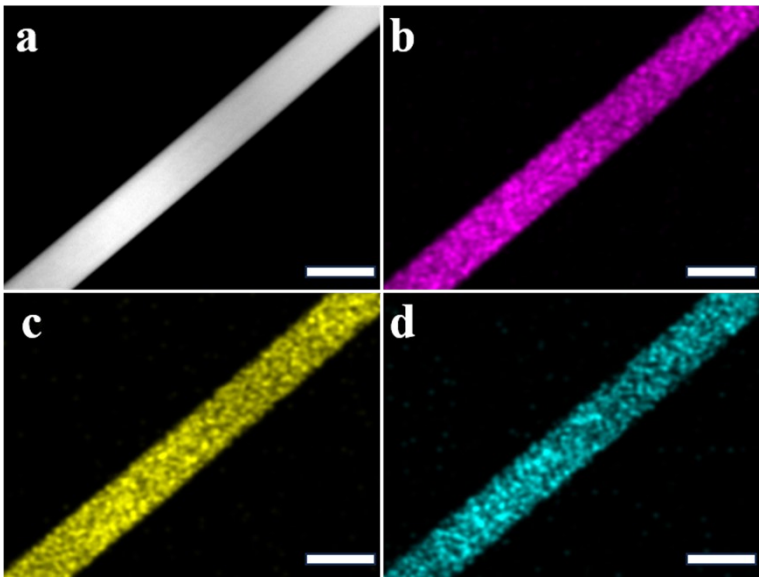

Fig. S6 (a) Low-magnification HAADF TEM image of a $Bi_2(Se,S)_3$ nanowire. Corresponding EDS element mapping of (b) Bi, (c) S and (d) Se element. The scale bar is 100 nm.

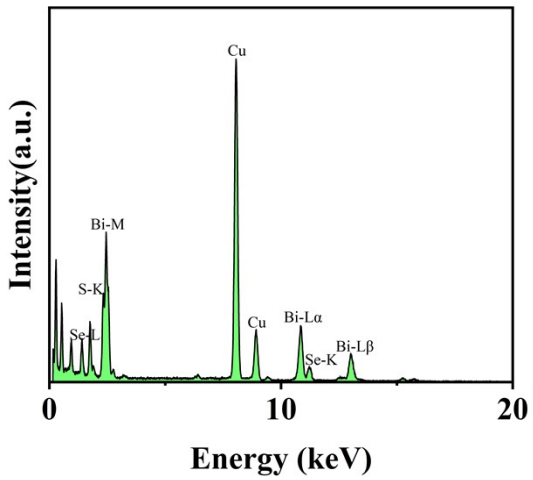

Fig. S7 EDS spectrum of the $Bi_2(Se,S)_3$ nanowire.

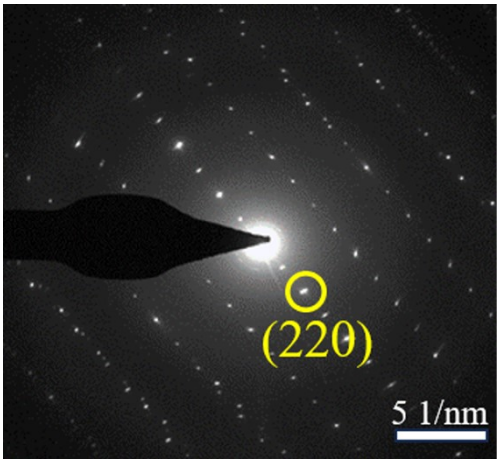

Fig. S8 SAED pattern of $Bi_2(Se,S)_3$ nanowires.

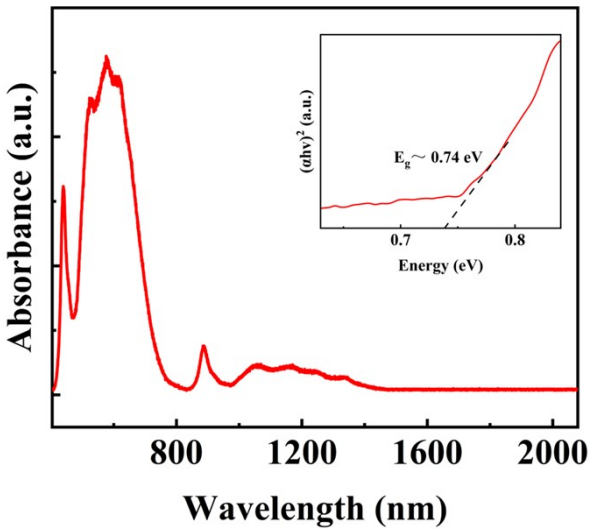

Fig. S9 Absorption spectrum of the $Bi_2(Se,S)_3$ nanowires. The insert is the plot of $(\alpha hv)^2$ versus energy of the exciting light.

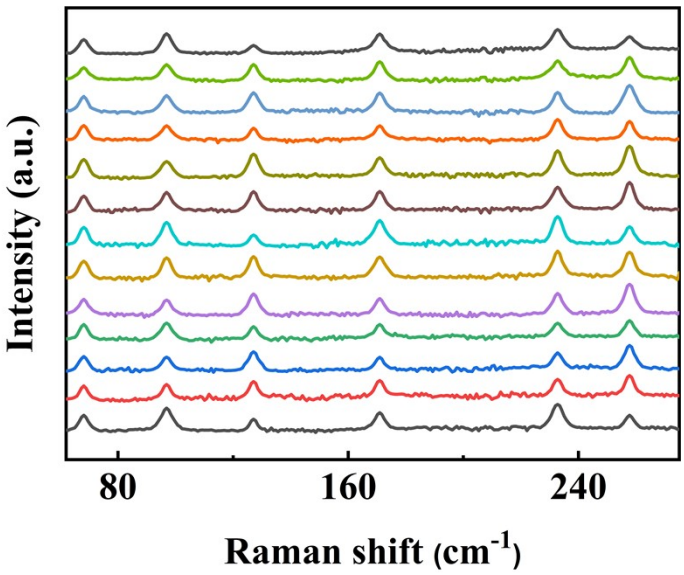

Fig. S10 The angle-resolved Raman scattering spectra under parallel configuration irradiated by 532 nm laser.

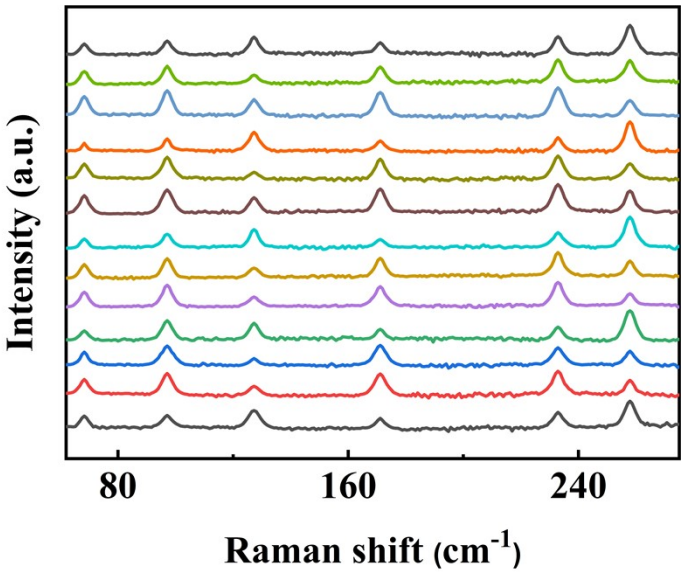

Fig. S11 The angle-resolved Raman scattering spectra under vertical configuration irradiated by 532 nm laser.

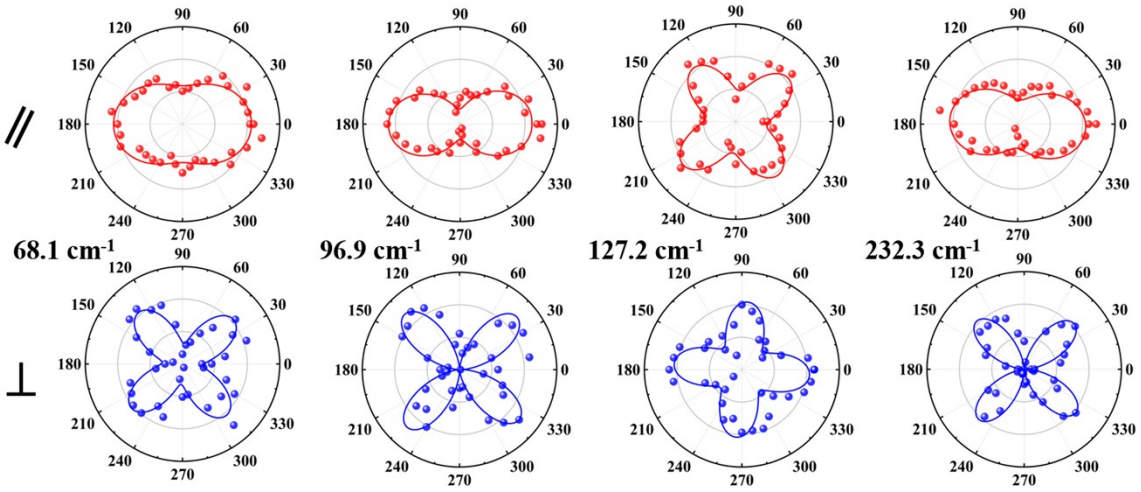

Fig. S12 The polar plots of angle-resolved Raman intensity corresponding to peak 68.1 cm^{-1}, 96.9 cm^{-1}, 127.2 cm^{-1} and 232.3 cm^{-1}, respectively under parallel (//) and cross configurations (⊥).

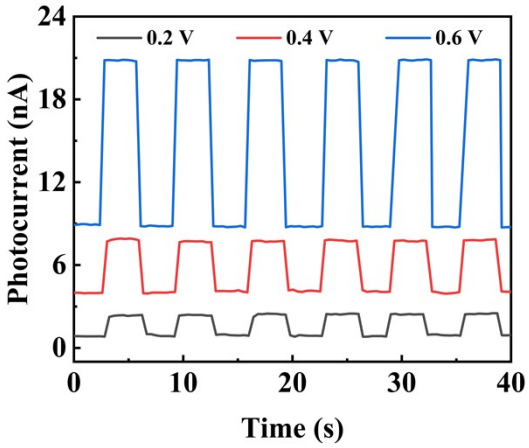

Fig. S13 Time resolved photoresponse of the device at different V_{ds}.

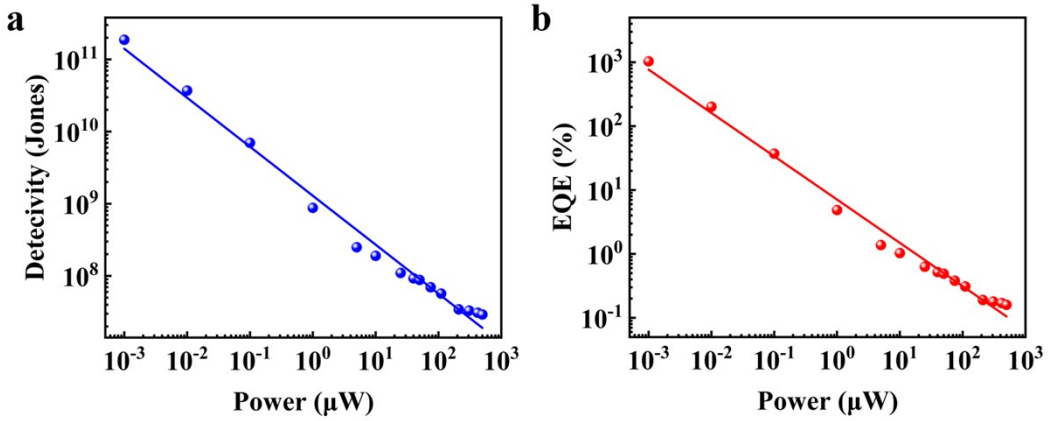

Fig. S14 (a) D^* and (b) *EQE* as function of light power intensity of the $Bi_2(Se,S)_3$ nanowire photodetector.

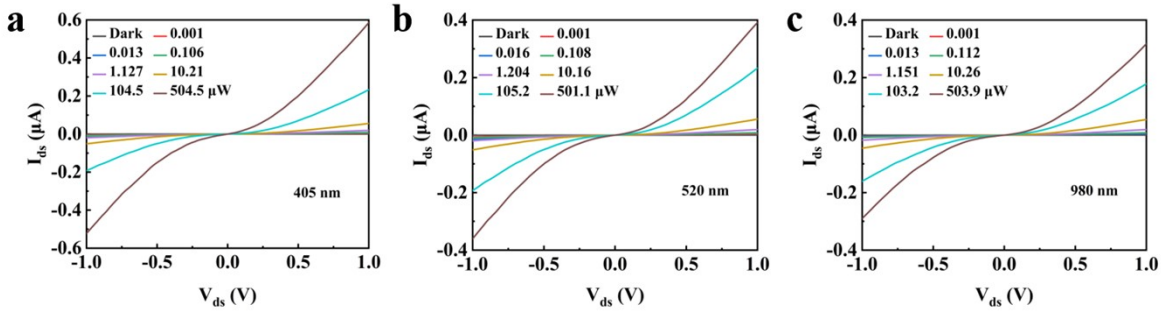

Fig. S15 The I_{ds}-V_{ds} curves of the $Bi_2(Se,S)_3$ nanowire devices under different laser wavelengths.

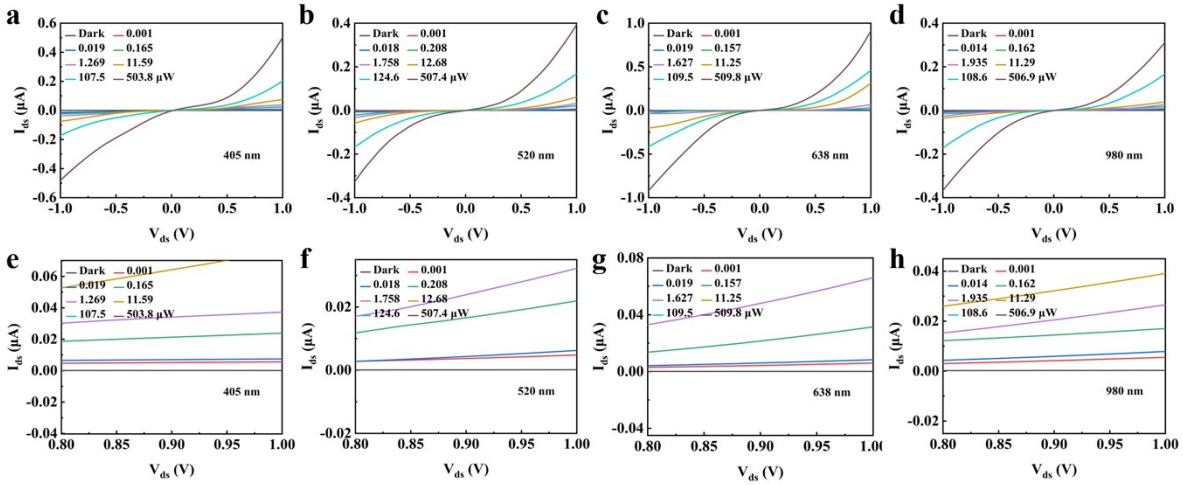

Fig. S16 The I_{ds}-V_{ds} curves of one $Bi_2(Se,S)_3$ nanowire device spin-coated with PMMA (device #1) under (a) 405 nm, (b) 520 nm, (c) 638 nm, and (d) 980 nm laser illumination. Local magnification of I_{ds}-V_{ds} curves under (e) 405 nm, (f) 520 nm, (g) 638 nm, and (h) 980 nm laser illumination.

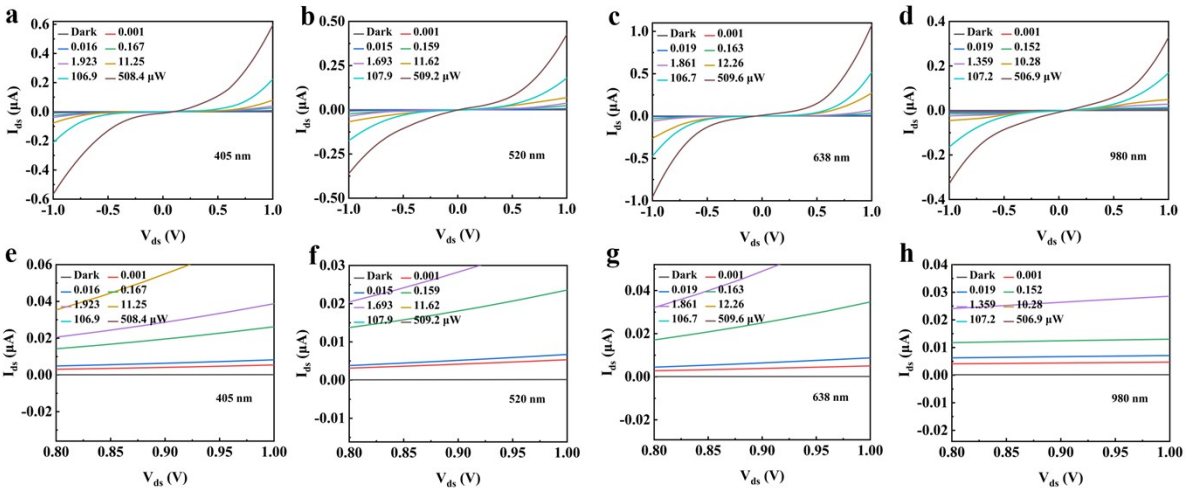

Fig. S17 The I_{ds}-V_{ds} curves of another $Bi_2(Se,S)_3$ nanowire device spin-coated with PMMA (device #2) under (a) 405 nm, (b) 520 nm, (c) 638 nm, and (d) 980 nm laser illumination. Local magnification of I_{ds}-V_{ds} curves under (e) 405 nm, (f) 520 nm, (g) 638 nm, and (h) 980 nm laser illumination.

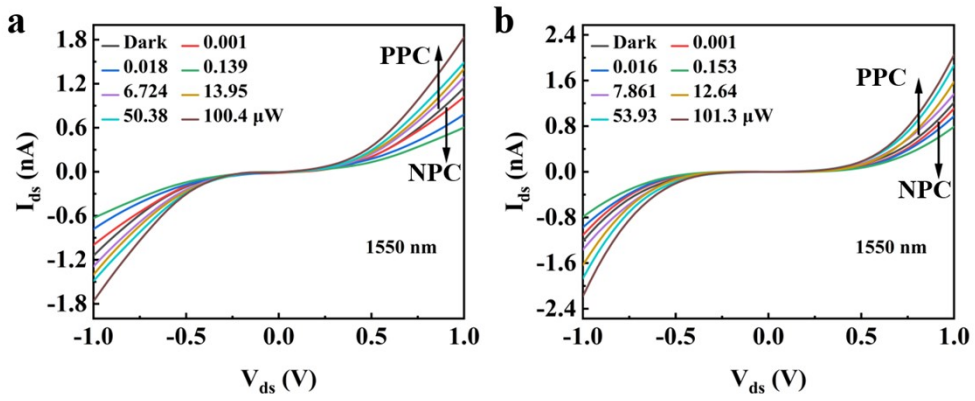

Fig. S18 The I_{ds}-V_{ds} curves of (a) device #1 and (b) device #2 under 1550 nm laser illumination.